Journal of Computational Physics **166,** 159–164 (2001)
doi:10.1006/jcph.2000.6643, available online at http://www.idealibrary.com on IDEAL®

NOTE

Accuracy Problems in Simulation of Field Emitter Devices Using Finite Elements

Albert Seidl* and Mikio Takai†

**Fachbereich Elektrotechnik, Fachhochschule Magdeburg, Breitscheidstrasse 2, 39114 Magdeburg, Germany; and †Research Center for Materials Science at Extreme Conditions, Osaka University, Machikaneyama 1-3, Toyonaka, Osaka 560-8531, Japan*
E-mail: albert.seidl@elektrotechnik.fh-magdeburg.de, takai@rcem.osaka-u.ac.jp

Received January 20, 2000; revised September 13, 2000

Key Words: simulation; Laplace equation; patch-test.

1. INTRODUCTION

The typical required accuracy of simulation results for engineering purposes is between 5% and 20%. The objective of electrical field calculations related to electronic devices is the prediction of electrical behavior, namely the voltage current characteristics. To maintain flexibility with space-charge effects or different dielectric materials in view, the finite element method (FEM) remains the method of choice for simulation of most kinds of devices. In resistance and capacitance calculations referring to capacitors, resistors, transistors, etc., the desired parameters can be extracted based on the energy balance, using computationally stable integration. In [1] it is shown that errors below 1% can be easily achieved using relatively coarse approximations in both the representation of the geometry and the discretization if not local field values but rather energy integrals are used to calculate resistance or capacitance. In the case of field emitter devices, however, the use of field strength obtained by estimating the local derivative of the potential cannot be avoided. In addition two effects act together to make the problem of field emitter devices especially critical:

- The device geometry exhibits large and small geometrical dimensions at the same time, which makes extreme local mesh refinement necessary.
- The local current density is related to the field strength via an exponential relationship (Fowler–Nordheim relationship [2–4]).

0021-9991/01 $35.00

In this paper the computational accuracy achieved by the finite element method is investigated experimentally. The criteria used are the convergence of solutions as local mesh refinement is improved and comparison with an analytical approximation. Two problems are common to analytical solutions used for technical tasks:

- They are valid for model geometries only with certain symmetry properties.
- Even for symmetric geometries they are applicable only if certain constraints on parameters are observed.

In spite of these shortcomings the analytical solution was found useful in characterizing the accuracy of the finite element computation.

2. THE PHYSICAL MODEL

The miniaturization of vacuum-electronic devices has become a new field of research within microsystems technology. A central point in recent research is the investigation of new mechanisms for current emission. Since devices using thermionic emission are difficult to realize on micrometer scale, emphasis is put on enhancing cold emission properties. The most critical aspect is the optimization of device geometry so that a high local electrical field is obtained. This is achieved by manufacturing devices that exhibit sharp edges. Mechanisms for electron emission are discussed elsewhere [2]. They lead to a relationship between the local electrical field and current density known as the Fowler–Nordheim relationship. This relationship is given by the formula

$$j(E) = \frac{AE^2}{\varphi \cdot t^2} e^{-B\nu(y)\phi^{3/2}/E}, \tag{1}$$

where

$$\nu(y) = \nu_0 - y_0^2 \frac{E}{\varphi^2},$$

and A, B, t, φ, ν_0, and y_0 are constants (e.g., [2]). Please note that current density $j(E)$ rises exponentially with the local electrical field strength E.

A typical field emitter geometry is sketched in Fig. 1. If E represents the surface of the emitter and G the surface of the gate, the PDE model can be summarized as follows [5]:

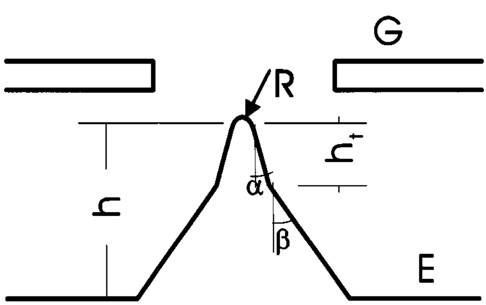

FIG. 1. Real-life emitter geometry. The structure is rotational symmetric with the dashed line as the symmetry axis. The shown ratio R/h does not represent a realistic geometry; it is typically less than 0.01. See [6, 7] for micrographs showing real-life devices.

Solve

$$\Delta\Phi = 0 \tag{2}$$

Dirichlet boundary conditions $\Phi = 0$ on E and $\Phi = V$ on G

Neumann boundary conditions on all other boundaries.

As outlined in [3] the resulting current I is obtained by integrating

$$I = \iint_S j(E)\, da \tag{3}$$

over the surface of the emitter tip, where the relationship $j(E)$ is given by Eq. (1).

3. THE FLOATING SPHERE EMITTER MODEL

The geometry shown in Fig. 1 can be simplified by making use of the fact that current emission takes place on the tip of the emitter only. The tip of the emitter is modelled by a floating sphere and the rest of the emitter is neglected. The resulting geometry is shown in Fig. 2. The question of whether this model is a good approximation of the real-life problem is not the subject of this paper. We have realized the model geometry using finite elements, thus allowing a direct comparison between analytical and numerical results. The expression needed for current integration is

$$E_{\mathrm{r}} = \frac{V}{d}\left(\frac{h}{R} + 3\cos\Theta\right). \tag{4}$$

This equation is frequently quoted in the literature on field emitters (e.g., [3, 8]), but the origin of the formula has not been clear up to now. Therefore it will be shown in the following how this equation is derived. A potential distribution can be constructed using a superposition of a linear and two sphere-symmetric contributions. The latter are solutions

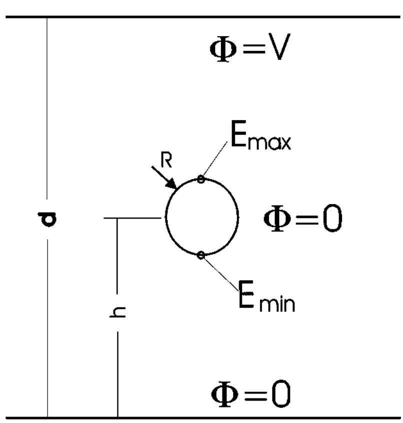

FIG. 2. Configuration of floating sphere emitter model with potential boundary conditions in comparison with a real-life geometry. Note that the exact shape of the upper electrode cannot be represented in the analytical model.

of the Laplace equation known as the point-charge and the point-dipole solution in spherical coordinates (e.g., [9]):

$$\Phi(r,\Theta) = \frac{V}{d}\left(h + r\cdot\cos\Theta - \frac{h\cdot R}{r} - \frac{R^3}{r^2}\cos\Theta\right). \tag{5}$$

By forming the partial derivative with respect to r and setting $r = R$ it can be easily shown that the electrical field, Eq. (4), is derived from this potential model. In order to check the boundary conditions, Eq. (5), we introduce the z-coordinate and eliminate Θ by substituting $z = h + r\cdot\cos\Theta$,

$$\Phi(r,z) = \frac{V}{d}\left(z - \frac{h\cdot R}{r} - \frac{R^3}{r^3}(z-h)\right). \tag{6}$$

It is obvious that the Dirichlet boundary condition $\Phi = 0$ cannot be satisfied exactly at the bottom plane ($z = 0$, $r = h$) by the point-charge and the point-dipole solutions, which exhibit spherical symmetry. By substituting the above-mentioned coordinate values we end up with a potential error on the order of magnitude $V\cdot R/h$. The same is true for the top plane. Therefore the expression for the electrical field is only an approximation and it is valid for $R \ll h$ and $R \ll d$ only. This condition is typically satisfied for field emitter devices with a total height of 1 μm and a tip radius of less than 10 nm.

4. RESULTS OF THE COMPUTATIONAL EXPERIMENT

Potential distributions for model problems were evaluated with different meshes using the ANSYS software. The values of field strength were computed for an applied voltage of 40 volts. A minimum mesh size was defined via a parameter R/d which determines the ratio of the radius of the emitter tip to the element size near the emitter. A coarser mesh was used in the other parts of the domain. Only the local mesh size near the emitter tip has been reduced in the critical region, leaving the rest of the mesh unchanged. A consistent reduction of mesh size is impractical due to existing limitations on problem size. By adjusting the boundary discretization a smooth transition from fine to coarse mesh could be achieved,

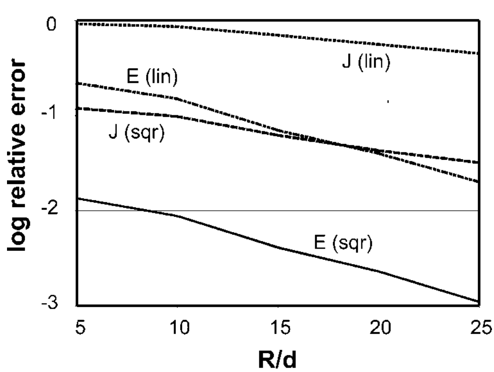

FIG. 3. Relative computational error as a function of the minimal mesh size for 4-node bilinear (lin) and 8-node second-order (sqr) elements. Achieved accuracies for field strength (E) and current density (J) are compared. The error of the analytical solution was 2.8×10^{-3} for the field strength and 5.1×10^{-2} for the current density.

TABLE I
Real-Life Configuration Computed with Different Sets of Mesh Parameters

Element Type	R/d	E_{max} [V/μm]	J_{max} [A/cm^2]
8-node, 2nd order PLANE121	62.5	1639.44	39
8-node, 2nd order PLANE121	31.2	1637.48	38
8-node, 2nd order PLANE121	15.6	1632.40	35
8-node, 2nd order PLANE121	7.8	1609.52	25
4-node, bilinear PLANE55	15.6	1496	4.4
4-node, bilinear PLANE55	7.8	1347	0.29

thus avoiding degenerate element shapes. The relative error ε_r was used as a measure for the computational accuracy,

$$\varepsilon_r = \frac{E_t - E}{E_t}, \tag{7}$$

where E_t denotes the “true” value of the field strength, and E the computed value. E_t was estimated by extrapolating the computed values of the last two mesh-refinement steps. The experiment was performed for a real emitter geometry (Fig. 1) and the floating sphere configuration (Fig. 2)

The computed values for the local field strength and current density of a real-life configuration (Fig. 1) are summarized in Table I, where the dependence of computed values for field strength and current density on the degree of local mesh refinement is demonstrated. Figure 3 shows the relative error depending on local mesh refinement for the floating sphere configuration (Fig. 2). Reasonable results were obtained for $R/d = 10$ or greater using second-order elements, which provided and accuracy of about 1% for the electrical field and 10% for the local current density. With a coarser discretization or lower order elements the error was over 10% for the electrical field and nearly 100% for the local current density. The error of the analytical solution was very small and comparable to the one obtained with a fine finite element mesh ($R/d = 20$).

5. CONCLUSION

It has been shown that the computation of the emission current of field emitters constitutes a particularly critical task for finite element electrical field calculations. It has been found experimentally that an acceptable accuracy of an FE solution can only be obtained by at least second-order elements together with extreme local mesh refinement. The floating sphere emitter model was shown to be an approximation for the simplified model geometry. However, if certain constraints on geometry parameters are observed, errors are small in comparison with the errors of coarse finite element results. Therefore the analytical approximation is a useful tool for calibration of the mesh generator. The analytical solution for the model problem, although not exact itself, can be utilized to identify an insufficient finite element solution.

ACKNOWLEDGMENTS

The authors thank Dr. Utsumi for valuable correspondence. One of the authors (A. S.) is indebted to Osaka University for providing the opportunity to carry out this work.

REFERENCES

1. A. Seidl, H. Klose, M. Svoboda, J. Oberndorfer, and W. Rösner, CAPCAL—A 3D capacitance solver for support of CAD systems, *IEEE Trans. CAD* **7**, 549–556 (1988).
2. I. Brodie and C. A. Spindt, Vacuum microelectronics, *Adv. Electron. Electron phys.* **83**.
3. D. Nicolaescu, Physical basis for applying the Fowler–Nordheim *J–E* relationship to experimental *I–V* data, *J. Vac. Sci. Technol. B* **11**, 392–395 (1993).
4. C. Constancias, *Emission d'electrons par effet de champ à partir de micropointes pour écrans plats: Simulations, caractérisations et confrontations expérimentales*, available at http://perso.libertysurf.fr/CONSTANCIAS/these_html/couverture.html.
5. Y.-J. Yang, F. T. Korsmeyer, V. Rabinowich, M. Ding, S. D. Senturia, and A. I. Akinwande, An efficient 3-dimensional CAD tool for field emission devices, in *Proceedings of IEDM 98* (1998), p. 863.
6. M. Takai, M. Yamashita, H. Wille, S. Yura, S. Horibata, and M. Ototake, Enhancement in emission current from dry-processed n-type Si field emitter arrays after tip anodization, *J. Vac. Sci. Technol. B.* **13**, 441–444 (1995).
7. A. Hosono, S. Yura, K. Morikawa, S. Kawabuchi, T. Okumura, S. Horibata, S. Okuda, H. Harada, and M. Takai, High current and stabilized field emitter arrays of tungsten-coated anodized silicon, in *Proceedings of IDW '96* (Kobe, 1996), Vol. 2, p. 531.
8. T. Utsumi, Keynote address. Vacuum microelectonics: What's new and exciting, *IEEE Trans. Electron Dev.* **38**, 2276 (1991).
9. Lautz, *Elektromagnetische Felder* (Teubner, Stuttgart, 1969).